



Title	Reactive interface formation and Co-induced (7×7) superstructure on a GaN(0001) pseudo- (1×1) substrate surface
Author(s)	Li, HD; Zhong, GH; Lin, HQ; Xie, MH
Citation	Physical Review B - Condensed Matter And Materials Physics, 2010, v. 81 n. 23
Issued Date	2010
URL	http://hdl.handle.net/10722/123857
Rights	Creative Commons: Attribution 3.0 Hong Kong License

Reactive interface formation and Co-induced $(\sqrt{7}\times\sqrt{7})$ superstructure on a GaN(0001) pseudo- (1×1) substrate surface

H. D. Li,¹ G. H. Zhong,² H. Q. Lin,^{2,3} and M. H. Xie^{1,*}

¹Physics Department, The University of Hong Kong, Pokfulam Road, Hong Kong, China

²Shenzhen Institutes of Advanced Integration Technology, Chinese Academy of Sciences, and The Chinese University of Hong Kong, Shenzhen 518055, China

³Physics Department, The Chinese University of Hong Kong, Shatin, Hong Kong, China

(Received 23 March 2010; revised manuscript received 11 May 2010; published 3 June 2010)

Deposition of Co on GaN(0001) pseudo- (1×1) surface at room temperature by molecular-beam epitaxy is studied by low-energy electron diffraction, scanning-tunneling microscopy and first-principles total energy calculations. Reactive interface formation where the deposited Co reacts with Ga on GaN substrate forming CoGa_x ($x\sim 2$) compound or alloy can be inferred from surface morphology evolution and mass consideration. At an intermediate coverage about 0.4 monolayers, a specific $(\sqrt{7}\times\sqrt{7})$ surface structural phase develops, as observed by both low-energy electron diffraction and scanning tunneling microscopy studies. First-principles total energy calculations suggest that the $(\sqrt{7}\times\sqrt{7})$ structure is induced by Co-trimers located slightly below the topmost Ga adlayer of the substrate.

DOI: [10.1103/PhysRevB.81.233302](https://doi.org/10.1103/PhysRevB.81.233302)

PACS number(s): 68.35.B-, 68.37.Ef, 68.47.Fg, 68.35.Md

Introduction. Heteroepitaxial growth of transition metals (TMs) on semiconductor substrates has been characterized by reactive interface formations, such as those on Si,¹⁻³ GaAs,⁴ InP,^{5,6} and InGaP.⁷ This is brought about by the strong chemical interaction between the TMs and semiconductors, and so instead of a simple epitaxial growth, radical rearrangements of surface atoms usually occur, giving rise to novel surface reconstruction and structures.^{8,9} In some cases, TMs destructively alloy with the substrate, giving rise not only to solid solutions but also to new phases of the materials.¹⁰⁻¹²

In the recent years, GaN has attracted a lot of attention for its short wavelength optoelectronic application.¹³ Efforts have been devoted to TMs deposition on GaN, such as Ni,¹⁴ Fe,¹⁵ and Mn,¹⁶ for interface properties and magnetism of ultrathin films. However, for GaN surface, complications exist owing to the various surface structures and compositions, depending on the preparation technique and conditions. Particularly, for GaN prepared by molecular-beam epitaxy (MBE) under excess Ga fluxes, the GaN(0001) pseudo- (1×1) (denoted hereafter by “ 1×1 ”) surface was found to be energetically stable as well as having smooth surface morphologies.^{17,18} The topmost Ga adatoms on GaN(0001)-“ 1×1 ” surface is not well ordered, rather they form a fluidlike layer being highly mobile and incommensurate with the GaN lattices.^{17,18} Therefore, it will not be surprising that the excess Ga may affect the formation and composition of the interface layers between TMs and GaN. Consequently, it is of great importance to examine the formation and evolution of the TMs/GaN interface for better understandings of magnetic properties of the heterosystems. It is also highly desirable to identify stable surface structure under various conditions for further development of growth techniques and strategies for high quality epitaxial TM films.

Here we present a study by low-energy electron diffraction (LEED) and scanning tunneling microscopy (STM) of Co deposition on GaN(0001)-“ 1×1 ” by MBE at room temperature. The reactive interface formation and evolution are followed. Combining with the first-principles total energy

calculations, the specific surface composition and structure is determined. It is evident that surface Ga adlayer on substrate participates in the interface formation. Depending on coverage, the surface evolves from an initial two-dimensional (2D) island nucleation, $(\sqrt{7}\times\sqrt{7})$ superstructure formation and finally to a degradation of the surface by nucleation of three-dimensional (3D) features. The $(\sqrt{7}\times\sqrt{7})$ surface is identified as due to a periodic arrangement of Co trimers located below the topmost Ga adlayer on surface. However, due to the much higher local density of states (LDOS) from Co, the Co-trimer gives rise to a bump in the STM image.

Experimental. The substrate (GaN) preparation, Co deposition, and subsequent LEED and STM experiments were conducted in a multichamber ultrahigh vacuum system with base pressures below 2×10^{-10} mbar. The substrate was commercial GaN/6H-SiC from TDI, Inc., on which a buffer film of approximately 300 nm thick was grown at $\sim 600^\circ\text{C}$ under excess Ga by MBE. The latter procedure produced the GaN(0001)-“ 1×1 ” surface, on which subsequent Co deposition was conducted in an adjacent MBE chamber. Typical morphology of the GaN(0001)-“ 1×1 ” surface was characterized by double bilayer (BL) steps ($1\text{ BL}=c/2\approx 2.6\text{ \AA}$, where c is the lattice constant along $[0001]$) delineating terraces of 50–100 nm wide. On a large length scale, however, the surface was seen to contain spiral mounds caused by preferential growth at screw dislocations.¹⁹ Co depositions on such surfaces were carried out at room temperature using an e-beam cell, where its flux was calibrated by a quartz crystal oscillator. Typical deposition rate was 0.01 MLs/s. Immediately after Co deposition for a specified coverage, the surface was examined by the LEED and STM *in situ* for surface structure and morphological information. For the former, diffraction patterns at different electron energies were taken, while for the latter, constant current mode of the STM was carried out at room temperature using the sample bias of -1.39 V and tunneling current of 0.1 nA.

Results and discussions. Figure 1(a) shows a relatively large-scale STM image depicting the morphology of the surface following ~ 0.14 MLs Co deposition on

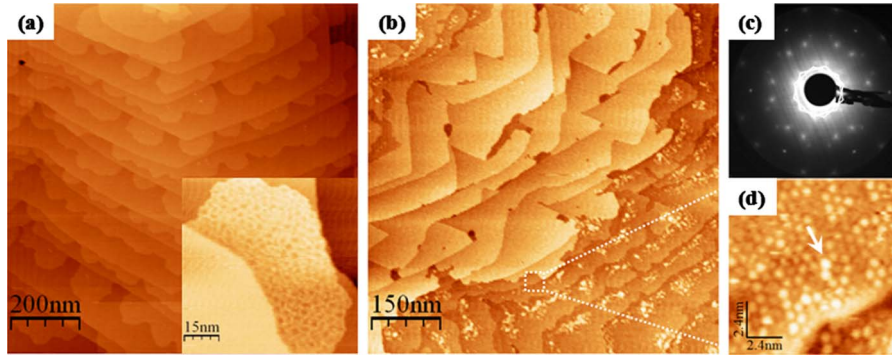


FIG. 1. (Color online) (a) STM image (size: $1000 \times 1000 \text{ nm}^2$) showing the surface of 0.14 MLs Co deposited on GaN(0001)-“ 1×1 .” The inset is a close-up image (size: $75 \times 75 \text{ nm}^2$) revealing surface corrugation on top of the 2D islands; (b) STM image (size: $750 \times 750 \text{ nm}^2$) of a surface following 0.4 MLs Co deposition; (c) LEED pattern taken from the surface of (b), where the solid and dashed hexagons highlight the $(\sqrt{7} \times \sqrt{7})R19.1^\circ$ and $(\sqrt{7} \times \sqrt{7})R-19.1^\circ$ reconstruction; (d) Close-up STM image (size: $50 \times 50 \text{ nm}^2$) of the rough surface region in (b), showing disordered atomlike clusters. The white arrow points at a seven atom ring.

GaN(0001)-“ 1×1 .” Besides the steps and terraces of the substrate, 2D islands as induced by Co deposition are seen to decorate the ascending steps on terraces. These islands are more or less circular in shape, while their STM contrast suggest an apparent height of $\sim 1.6 \text{ \AA}$, which is slightly less than expected from a hexagonal close packed (hcp) Co atomic layer ($\sim 2.0 \text{ \AA}$). The total coverage of the islands as measured by STM is about 0.42 MLs, three times that of the deposited coverage. So, it seems that the islands are not composed solely of Co atoms. The additional mass must be from the substrate and thus a reactive surface/interface formation takes place. Given that the GaN(0001)-“ 1×1 ” substrate surface contains excess Ga adlayers, it is likely that the deposited Co has reacted with Ga, forming CoGa_x ($x \sim 2$) during the initial stage nucleation of islands. Indeed, from the phase diagram of the Co-Ga system, CoGa_x compound or alloy can be thermodynamically favorable at room temperature.²⁰ Close-up images of the islands such as that shown in the inset in Fig. 1(a) reveal morphological corrugations, while the LEED experiments do not reveal any satellite diffraction spots. Therefore, the corrugated morphology in STM may suggest a random chemical distribution pertinent to CoGa_x alloys.

As the nominal coverage of Co is increased to above 0.2 MLs, a striking surface structural phase transition occurs. Instead of random alloy, an ordered structure with $\sqrt{7} \times \sqrt{7}$ translational periodicity emerges, as evident from both STM and LEED experiments. Such ordered feature becomes prominent at the deposition coverage of ~ 0.4 MLs of Co. Figure 1(b) shows a STM micrograph depicting the surface following deposition of 0.4 MLs of Co. One notes that the surface is dominated by regions of smooth morphology with brighter contrast, though there are also areas showing relatively a rough morphology, containing some 3D features surrounded by less bright and seemingly corroded terraces, as shown in Fig. 1(b) at the lower right. Zooming in the smooth surface region reveals domains of ordered structures of Fig. 2, which can be characterized as the $\sqrt{7} \times \sqrt{7}$, except with $\sim 6.4\%$ size contraction with respect to the ideal size of $7a_{\text{GaN}}^2$. The $\sqrt{7} \times \sqrt{7}$ superstructure is confirmed by the LEED as shown in Fig. 1(c), where two sets of satellite diffraction spots are observed, suggesting coexistence of two rotational

domains. With reference to the diffraction patterns from GaN(0001) substrate surface, we may infer the two rotational domains as $(\sqrt{7} \times \sqrt{7})R19.1^\circ$ and $(\sqrt{7} \times \sqrt{7})R-19.1^\circ$, respectively. Such rotational domains can also be noted from the STM images, such as that of Figs. 2(b) and 2(c), obtained from different regions of the same surface. In the LEED, one also notes the satellite diffraction spots are rather diffusive. This indicates small areas even for the same rotational domains, which is also apparent from the STM image (Fig. 2). Indeed, domain walls composed of missing atoms are abundant in Fig. 2. Rows of “atoms” are seen to spatially shift by $\sim 2.8 \text{ \AA}$, i.e., $1/3$ of the $\sqrt{7} \times \sqrt{7}$ unit cell size when crossing the domain boundaries. Some of these translational misaligned “atom rows” are marked by the solid and dashed white lines in Figs. 2(b) and 2(c). As for the rough surface region in Fig. 1(b), some 3D island features have developed, which are accompanied by corruptions of the terraces, particularly in areas close to the ascending steps. A close-up STM images in such areas still show the atomlike clusters,

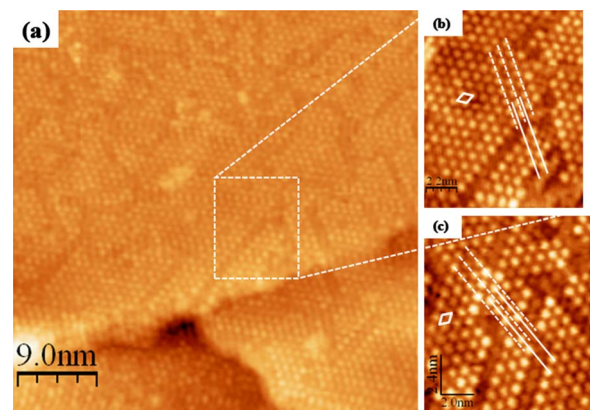


FIG. 2. (Color online) (a) Close-up STM image (size: $45 \times 45 \text{ nm}^2$) of the smooth surface region in Fig. 1(b), showing domains of the ordered $(\sqrt{7} \times \sqrt{7})$ structure on surface. [(b) and (c)] Zoom-in STM images (size: $10 \times 12 \text{ nm}^2$) at different locations of the smooth surface area, revealing rotational and translational domains of the $(\sqrt{7} \times \sqrt{7})$ superstructure. The rhombus indicate unit cell of the structure, while the solid and dashed lines mark atom rows showing their misalignment when crossing domain boundaries.

though they are not well ordered. One of such close-up images is shown in Fig. 1(d), from which clusters comprising one or few atoms, some arranged in the $\sqrt{7} \times \sqrt{7}$ structure while others in some peculiar ways are found. For example, ringlike clusters are observed in Fig. 1(d), as pointed by white arrows.

Superstructures induced by metal deposition on semiconductors have, in fact, been reported for a number of heterosystems,^{21,22} including that on GaN(0001)-“ 1×1 ” surface.^{16,17,23} Co-induced ringlike structure was also observed on Si(111) upon high-temperature annealing of the $\sqrt{7} \times \sqrt{7}$ structured surface,⁸ where low density of isolated ring-clusters and small domains of $\sqrt{7} \times \sqrt{7}$ structure coexisted on the surface. The $\sqrt{7} \times \sqrt{7}$ superstructure was identified to be of single Co atom surrounded by six Si adatoms.⁸ In this study, we observe the ring cluster without invoking the annealing procedure and the $\sqrt{7} \times \sqrt{7}$ superstructure is more likely to be associated with Co trimers rather than Co monomer, as will be discussed in detail below. Noting that there is $>20\%$ lattice mismatch between Co and GaN lattices, by forming a unique domain structure with missing atoms in domain walls, the misfit strain has been effectively reduced to $\sim 6.4\%$. Formation of domains of superstructures on semiconductor surfaces upon transition-metal deposition seems rather general, reflecting the unique property of such heteroepitaxial systems.

In the following, we examine the ordered $\sqrt{7} \times \sqrt{7}$ structure of Co/GaN(0001)-“ 1×1 ” surface in more detail. Since the LEED pattern shows the strongest satellite spots pertinent to the ($\sqrt{7} \times \sqrt{7}$) structure at ~ 0.4 MLs coverage, which would correspond to that of the whole surface being of such a structure, the number of Co atoms within each of the $\sqrt{7} \times \sqrt{7}$ unit cell would be $0.4 \times (\sqrt{7} \times \sqrt{7}) \approx 3$. In other words, each bright “atomlike” feature in the STM image of Fig. 2 may be a reflection of 3 Co atoms, or a Co-trimer, rather than a single Co-monomer, as the latter would suggest a Co coverage of $1/(\sqrt{7} \times \sqrt{7}) \approx 0.14$ MLs only. This is similar to the case of the initial 2D islands nucleated in the very initial stage deposition, where the total island area corresponds to three times the mass of the deposit from flux [Fig. 1(a)].

Modeling and total energy calculations. To show that such a Co-trimer assumption is viable and to identify the specific atomic arrangements of the surface atoms, first-principles total energy calculations employing the projected augmented wave method^{24,25} as implemented in Vienna *Ab initio* simulation package (VASP) were performed.^{26,27} The exchange-correlation interaction was treated as the generalized gradient approximation (GGA) of Perdew-Burke-Ernzerhof (PBE) version.²⁸ To ensure the numerical convergence, the plane-wave expansion had a large energy cutoff of 500 eV, while the reciprocal space was sampled by $5 \times 5 \times 1$ k points in the Monkhorst-Pack grids. The GaN(0001)-“ 1×1 ” surface structure was modeled with periodically repeated slabs consisted of six layers of GaN and laterally contracted Ga bilayers on top, and the slabs are separated by a 10 Å vacuum region. One side of the slab was saturated with hydrogen atoms of fractional charge. Co-monomer and Co-trimer absorption on different high symmetry sites of the surface, such as the H3, T4, and the top T1 sites, were considered. The surface unit cells have a ($\sqrt{7}$

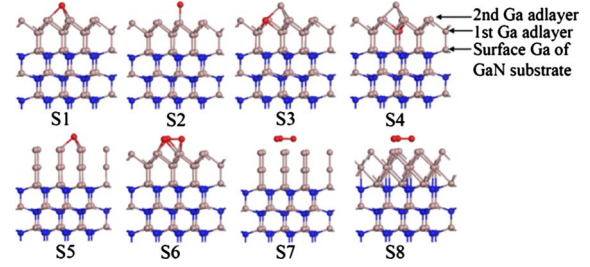


FIG. 3. (Color online) Models of Co-monomer (S1-S5) and Co-trimer (S6-S8) absorption/incorporation in a Ga-bilayer covered GaN(0001) surface. The brown (gray), blue (dark), and red (dark gray) balls represent Ga, N, and Co atoms, respectively.

$\times \sqrt{7}$) periodicity. Atoms of the top three GaN bilayers, the Ga adlayers and the absorbed Co were allowed to relax until the residual forces on each atom became smaller than 0.03 eV/Å and the total energy difference between two adjacent steps was smaller than 10^{-5} eV. Relative formation energy, E_f , of the various configuration were calculated, and the E_f is defined as^{29,30}

$$E_f = E - E_{\text{ref}} - \Delta n(\text{Ga})\mu_{\text{Ga}} - \Delta n(\text{N})\mu_{\text{N}} - \Delta n(\text{Co})\mu_{\text{Co}} - \Delta n(\text{H})\mu_{\text{H}} \quad (1)$$

where E is the total energy of the configuration under consideration, E_{ref} is the total energy of the reference configuration chosen to be the most stable one as shown later. μ_i ($i = \text{Ga, N, Co, and H}$) is the chemical potential of the i th species, and $\Delta n(i)$ is the excess or deficit of atoms of the i th element relative to that of the reference. The formation energy is calculated as a function of Co chemical potential in the range of $\mu_{\text{Co}}(\text{atom}) \leq \mu_{\text{Co}} \leq \mu_{\text{Co}}(\text{bulk})$, where $\mu_{\text{Co}}(\text{atom})$ and $\mu_{\text{Co}}(\text{bulk})$ are the chemical potentials when Co exists in the form of an isolated atom or bulk, respectively.

In view of the above STM observation, Co-trimer absorption as well as Co monomer is considered. Examples of the considered absorption configurations are illustrated in Fig. 3. They include a Co-monomer or Co-trimer per ($\sqrt{7} \times \sqrt{7}$) cell being absorbed on the Ga-bilayer covered GaN(0001) surface (S1, S2, S5-S8), Co atoms incorporated in the Ga adlayer (S3, S4), etc. Besides considering Co absorption at different high-symmetry surface sites, different atomic arrangement of the Ga atoms in the adlayers are also examined. For examples, Ga atoms in the first Ga adlayer can be directly on top of the surface Ga of GaN(0001) substrate while the second (top) Ga-adlayer atoms are stacked in the face-centered cubic (fcc), hexagonal closed packed (hcp) or on-top configurations (S1-S7 in Fig. 3). This is because the Ga in the top adlayer are mobile, being fluidlike according to some previous investigations.^{17,18} For completeness, some other configurations such as that shown in S8 of Fig. 3 where the Ga atoms in the first and second adlayers are fcc or hcp stacked with respect to GaN(0001), are also examined. Figure 4 shows the calculated relative formation energies of the various configurations as a function of μ_{Co} [relative to $\mu_{\text{Co}}(\text{bulk})$]. Structural optimization of Co-monomer absorbed surfaces suggests that the Co atom preferentially incorporates into and stay slightly below the topmost Ga adlayer. The most favorable configuration after atom relaxation has a

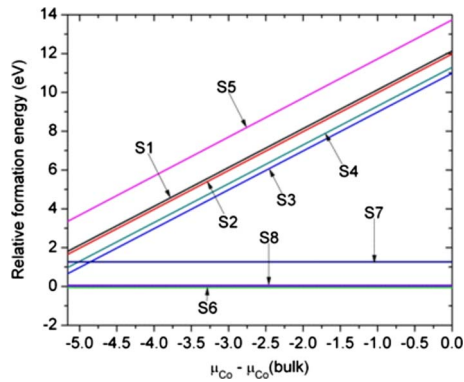


FIG. 4. (Color online) Relative formation energies of the various configurations after atom relaxation from those shown in Fig. 3, which are plotted as a function of the relative chemical potential of Co.

formation energy that is ~ 0.67 eV more than that of the reference model containing a Co trimer (model S6). Figures 5(a) and 5(b) show, respectively, the top and side views of the stabilized configuration of atoms after a Co-trimer is absorbed on Ga(0001)-“ 1×1 ” surface. It is shown that the three Co atoms are located slightly below the topmost Ga adlayer, and each of the three Co atoms is located at T4 site. Atom relaxation of model S8 has resulted in a stabilized structure similar to Figs. 5(a) and 5(b), except that the topmost Ga atoms are at the T4 sites while the Co atoms are at the H3 sites. So the two cases where the Co atoms are at either the H3 or T4 sites are energetically degenerate. The topmost Ga adlayer appears crinkled and contracted and the surface shows a slight depression (~ 0.7 Å) at the Co-trimer sites. However, the local density of states (LDOS) near the Fermi level [Fig. 5(c)] is significantly higher at Co sites than at Ga. Therefore, despite being spatially lower than Ga, the Co trimer will show up as bumps in STM micrographs. The ($\sqrt{7} \times \sqrt{7}$) superstructure thus reflects periodic arrangements of Co trimers on surface, where each of the atomlike feature in Fig. 2 is a Co trimer rather a single Co-monomer, which supports the assignment based on coverage considerations.

Summary. To summarize, absorption of Co on

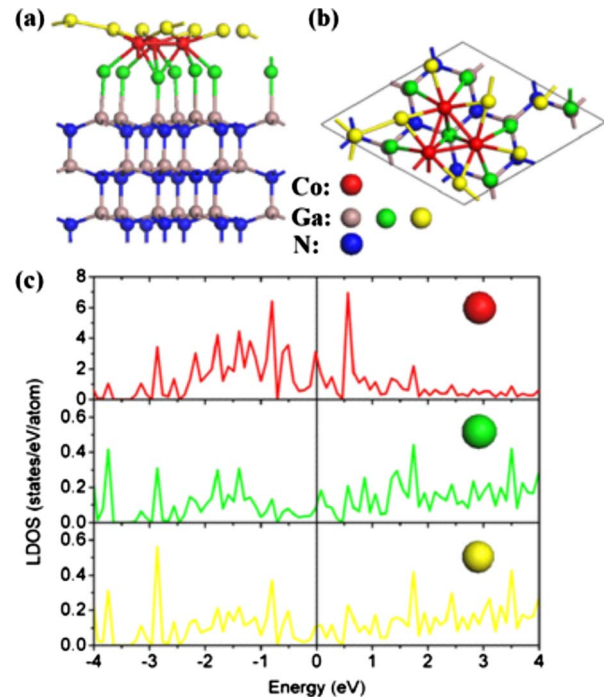


FIG. 5. (Color online) [(a) and (b)] Side and top views of the most favorable configuration of atoms containing a Co-trimer in the ($\sqrt{7} \times \sqrt{7}$) cell. The brown, green, and yellow balls represent Ga atoms in GaN surface, the first and second Ga adlayers, respectively. The blue balls are N atoms, and the red balls are Co. (c) Calculated LDOS at Co sites, the first and second Ga-adlayer atoms, respectively.

GaN(0001)- “ 1×1 ” surface at room temperature involves Co-Ga interaction, so instead of a metallic Co layer, CoGa_x ($x \sim 2$) compound or alloy form. This is reflected both at the very initial stage islands nucleation and at intermediate coverage formation of the $\sqrt{7} \times \sqrt{7}$ superstructure. Such an effect would have important implications in future studies of magnetism of such heteroepitaxial thin films.

We acknowledge the financial support of the NSFC/RGC Joint Research Scheme under Grant No. N_HKU705/07.

*Corresponding author; mhxie@hkusua.hku.hk

- ¹C. Pirri *et al.*, *Phys. Rev. B* **30**, 6227 (1984).
- ²J. Derrien *et al.*, *Phys. Rev. B* **36**, 6681 (1987).
- ³J. Y. Veuillein *et al.*, *Appl. Phys. Lett.* **51**, 1448 (1987).
- ⁴J. J. Krebs *et al.*, *J. Appl. Phys.* **61**, 2596 (1987).
- ⁵T. Kendelewicz *et al.*, *Phys. Rev. B* **34**, 558 (1986).
- ⁶C. M. Aldao *et al.*, *Phys. Rev. B* **37**, 6019 (1988).
- ⁷K. Ludge *et al.*, *J. Vac. Sci. Technol. B* **21**, 1749 (2003).
- ⁸P. A. Bennett *et al.*, *Phys. Rev. Lett.* **69**, 1224 (1992).
- ⁹M. A. K. Zilani *et al.*, *Phys. Rev. B* **72**, 193402 (2005).
- ¹⁰A. E. Dolbak *et al.*, *Surf. Sci.* **373**, 43 (1997).
- ¹¹H. S. Venugopalan *et al.*, *J. Appl. Phys.* **82**, 650 (1997).
- ¹²K. Ludge *et al.*, *J. Vac. Sci. Technol. B* **20**, 1591 (2002).
- ¹³J. I. Pankove and T. D. Moustakas, *Gallium Nitrides(GaN) I* (Academic Press, San Diego, 1998), Vol. 50; *Gallium Nitrides(GaN) II* (Academic Press, San Diego, 1999), Vol. 57.
- ¹⁴V. M. Bermudez *et al.*, *Phys. Rev. B* **48**, 2436 (1993).

- ¹⁵K. He *et al.*, *Appl. Phys. Lett.* **88**, 232503 (2006).
- ¹⁶Y. Cui and L. Li, *Surf. Sci.* **522**, L21 (2003).
- ¹⁷A. R. Smith *et al.*, *J. Vac. Sci. Technol. B* **16**, 2242 (1998).
- ¹⁸J. E. Northrup *et al.*, *Phys. Rev. B* **61**, 9932 (2000).
- ¹⁹H. Zheng *et al.*, *Phys. Rev. B* **77**, 045303 (2008).
- ²⁰J. Grobner *et al.*, *J. Phase Equilib.* **20**, 615 (1999).
- ²¹D. M. Chen *et al.*, *Phys. Rev. Lett.* **61**, 2867 (1988).
- ²²J. Zegenhagen *et al.*, *Phys. Status Solidi B* **204**, 587 (1997).
- ²³Y. Qi *et al.*, *Appl. Phys. Lett.* **92**, 111918 (2008).
- ²⁴P. E. Blöchl, *Phys. Rev. B* **50**, 17953 (1994).
- ²⁵G. Kresse and D. Joubert, *Phys. Rev. B* **59**, 1758 (1999).
- ²⁶G. Kresse and J. Furthmüller, *Comput. Mater. Sci.* **6**, 15 (1996).
- ²⁷G. Kresse and J. Furthmüller, *Phys. Rev. B* **54**, 11169 (1996).
- ²⁸J. P. Perdew *et al.*, *Phys. Rev. Lett.* **77**, 3865 (1996).
- ²⁹G.-X. Qian *et al.*, *Phys. Rev. B* **38**, 7649 (1988).
- ³⁰J. E. Northrup and S. B. Zhang, *Phys. Rev. B* **47**, 6791 (1993).